15 Contribution by SPTU: Support of Partners' Efforts Directed to Implementation of DES Technology

A. Garbaruk, D. Magidov, M. Shur, M. Strelets, and A. Travin
St.-Petersburg State Technical University (SPTU)

Abstract

This chapter summarises the work performed by St.-Petersburg State Technical University as a major sub-contractor in FLOMANIA. Along with a support of Partners' work on implementation of the Detached-Eddy Simulation methodology (DES) being the main responsibility of SPTU within FLOMANIA, this includes some own DES and RANS studies carried out on requests of the Project coordinator.

15.1 Introduction

SPTU has occupied a central position in efforts to exploit DES by the other Partners within FLOMANIA that had been a long-term goal of the Project. This has resulted in a large number of SPTU interactions with different Partners, mostly concerned with different aspects of implementation and tools for analysis of LES and DES simulations. Other than that, SPTU provided meshes for DES of NACA 0012 airfoil beyond stall (Test Case 14) and 3D Circular Cylinder (Test Case 21) and performed DES of these and some other generic test cases that were used by the other Partners for validation of DES implementations in their in-house CFD codes.

Along with this, SPTU has provided a support to the interested Partners in implementation of the SARC turbulence model of Spalart and Shur, 1997 and performed RANS computations of several test cases (9, 14, 26, 28) with the use of the conventional linear eddy viscosity models (SA, SARC, SST). This activity has permitted to widen the comparison of different models capabilities as applied to complex turbulent flows.

Finally, an important outcome of SPTU participation in FLOMANIA the university has significantly benefited from, is an implementation and validation of the Common Differential Reynolds Stress Model (SSG-Ch) in the in-house code (NTS code).

Below we first briefly outline this code, which has been used by SPTU in all the numerical studies (Section 15.2). Then, in Section 15.3, we highlight some results of SPTU activity in DES area. Finally, in Section 15.4, results are presented of the 3D RANS computations of the A-airfoil aimed at the evaluation of 3D-effects caused by the sidewalls of the test section in the experiment.

15.2 NTS Code Description

The NTS computer code is solving 2D and 3D, compressible (arbitrary Mach number) and incompressible, steady and time-dependent Navier-Stokes equations with the use of a high-order implicit finite-volume formulation on the structured

multi-block overlapping grids. Turbulence treatment is possible in the framework of the steady and unsteady RANS with a wide variety of conventional statistic turbulence models as well as with "turbulence resolving" approaches such as DES (based on SA and SST RANS models), LES, and DNS.

Following implicit flux-difference splitting numerical methods (based on MUSCL approach) are implemented in the code.

1. Method of Rogers and Kwak, 1988 (for incompressible flows).
2. Method of Roe, 1981 (for compressible flows).
3. Method of Weiss and Smith, 1995 with low Mach number preconditioning (for compressible flows at arbitrarily low Mach number).

Spatial approximation of the inviscid fluxes within all these methods is performed with the use of 3rd or 5th-order upwind-biased scheme or with the use of 4th-order centered scheme. Also, hybrid, weighted upwind/centered, schemes with the blending function dependent on the solution (Travin et al., 2002) or specified by the user are available and routinely used in DES, LES, or DNS. For the supersonic flows with shocks, flux limiting with a range of standard limiters can be turned on in order to provide smooth solutions in the vicinity of shock waves.

Viscous fluxes are approximated with the 2nd-order (default) or with the 4th–order (optionally) centered schemes.

Time integration in the code is implicit, with user-specified type of relaxation procedure including Gauss-Seidel relaxation by planes/lines, LU relaxation, or diagonally dominant approximate factorization (DDADI). Optionally, different implicit algorithms can be used in different grid blocks and, also, for solution of the gas-dynamic and turbulence-transport equations.

For the unsteady flows, time-derivatives are approximated with 2nd-order backward differences (three-layer scheme) with dual time-stepping (infinite default pseudo-time step) and sub-iterations. The number of sub-iterations at each time step depends on the problem being solved but usually is within the range from 5 up to 20 (this ensures reduction of the maximum residual by 3-4 orders of magnitude).

Parallelization of the solver is based on a "hybrid" conception that combines MPI and Open MP technologies. This permits to adjust the code to a specific hardware being used (shared, distributed or mixed memory structure).

It should be noted that the code permits computations with structured grid-blocks being not only simple rectangular parallelepipeds (in the computational coordinates) but also with the blocks containing arbitrary "holes" (cut-outs) inside such parallelepipeds. This feature is very helpful since it permits to minimize the number of the inter-block boundaries.

The inter-block interaction is implemented as follows. It is assumed that the grid-blocks used are the overlapping (not simply adjacent) ones. Coupled with the iterative procedure used for the solution of both steady-state and time-dependent problems, this permits to avoid imposing of any artificial boundary conditions at the inter-block boundaries. Namely, at each global iteration (for the steady problems) or at each subiteration of a time-step (for the time-accurate simulations), the values of all the primary variables (pressure, velocity

components, and temperature) at the inter-block boundaries of a recipient block are computed by interpolation over the neighbouring cells of the donor grid-block. At the implicit stage of the solution procedure, zero values of all the residuals are imposed at the inter-block boundaries. In case of multiple blocks overlapping, a special system of priorities is applied to choose the block for interpolation. Other than that, an algorithm is developed that does not cause any lowering of the order of the spatial approximation in the case when the grids of the neighbouring blocks in the overlapping region are identical (a converged solution is the same as that obtained on a single-block grid). This feature is very important for parallel computations on computers with distributed memory, when the grid is being subdivided into several blocks artificially, i.e., only in order to provide a possibility for MPI-parallelization, since it permits to avoid any decrease of accuracy in this case.

The code has been intensively employed for many years now. A list of applications include a wide range of RANS, URANS, DES and DNS of aerodynamic flows and, also, LES-based computations of the jet noise. Accumulated experience shows that independently of the type of the flow through the boundary (subsonic or supersonic) the approach briefly outlined above does not virtually cause slowing down of the iterations convergence versus similar single-block computations, provided that the grid-steps in the overlapping regions are close to each other, and the overlapping is “deep” enough (more than one grid cell). Other than that, no noticeable defects of solutions are observed in the vicinity of the block interfaces. This is essential for the highly unsteady flows with vortices crossing the boundary, which is inevitable in any turbulence-resolving simulations (DES/LES/DNS).

15.3 Major Results of Activity in DES Area

15.3.1 Support of Partners in Implementation of DES

As mentioned in the Introduction, in accordance with its role in the Project, SPTU had a large number of interactions with different partners aimed at sharing experience in the area of DES.

First of all, software for calibration of the subgrid scale models for DES has been transferred to the partners with appropriate running and post-processing instructions. The software is a code generating a random divergence-free velocity field with a prescribed turbulence kinetic energy spectra needed to initiate simulation of decaying homogeneous isotropic turbulence in a cubic box with fully periodic boundary conditions. It also includes a post-processing routine for computing the energy spectrum by a given velocity field.

Further support was provided in a form of advices and comments on the implementation and verification of the DES technology in partners’ in-house codes. Specifically, SPTU has provided statements and solutions for several test cases (backward facing step flow, the NACA0012 airfoil beyond stall (TC16)) to verify the implementation of the methodology. This includes a complete description of boundary conditions, meshes, pre- and postprocessing software, and supplementary information on numerical and implementation details.

Other than that, a current version of an empirical function designed to provide an automatic smooth switch from a high-order upwind-biased scheme in the RANS and irrotational regions of DES to central differencing in LES regions was distributed to the interested partners. On the basis of the suggested blending-function, AEA has developed a variant approach suited to CFX software.

Finally, in the course of a visit to TUB, Prof. M. Strelets gave a talk on DES fundamentals and applications. In the course of the visit to DLR, Dr. M. Shur provided assistance in implementation of the SA DES model in DLR's in-house CFD code TAU. In the course of a visit to IMFT, Prof. M. Strelets and Dr. M. Shur provided to IMFT background information on DES and some practical recommendation on its numerical implementation. Furthermore, SPTU interacted systematically with IMFT and provided some suggestions on the implementation of the DES technique in the IMFT codes. Much of this interaction was also devoted to an investigation of several aspects of the IMFT test case of flow around a circular cylinder (TC 21).

15.3.2 DES of 3D Circular Cylinder (IMFT Test Case 21)

The experimental study of this flow has been carried out by IMFT. A circular cylinder is placed in the 2,40m length test-section of S1/IMFT's subsonic wind tunnel between two end plates so that the cylinder aspect ratio, $L/D = 4.8$ (L is the distance between the two end-plates, D is the diameter of the cylinder) and the blockage ratio, $D/H=0.208$ (H is the distance between of the upper and lower walls of the section). The Reynolds number of the flow based on the cylinder diameter and inlet velocity was 140,000.

Preliminary, coarse grid, DES of the flow based on the assumption that the regime is sub-critical (laminar boundary layer separation and transition to turbulence in the separated shear layer) has shown that the boundary layers forming on the side-plates are very thin and do not affect the "core" of the flow any significantly. This is seen in Fig. 1, where we present an instantaneous swirl isosurface and the averaged pressure field from this simulation: the results visually reveal thin sidewall boundary layers and extended "2D" core. This finding has justified a much less expensive simulation with account of the upper and lower walls only, needed to represent their blocking effect, with the use of the periodic boundary conditions in the spanwise direction (two runs have been carried out with the span-period, L_z, equal to 2 and 4 cylinder diameters). A comparison of the results obtained in the simulations with the IMFT experimental data is presented in Figs.2-4. One can see that both mean flow velocity and turbulence statistics (Reynolds stresses) from the simulation agree with the data fairly well. It should be noted, that initially, due to some inconsistency in the pressure measurement technique, the experimental surface pressure significantly deviated from the predicted one. Exactly this circumstance gave a motivation to a double-checking of the experimental procedure by IMFT, which resulted in the correction of the original measurements (exactly these, corrected, data are presented in Fig. 4). Thus, this study provides an example of "validation of experiment by CFD" being far from typical today.

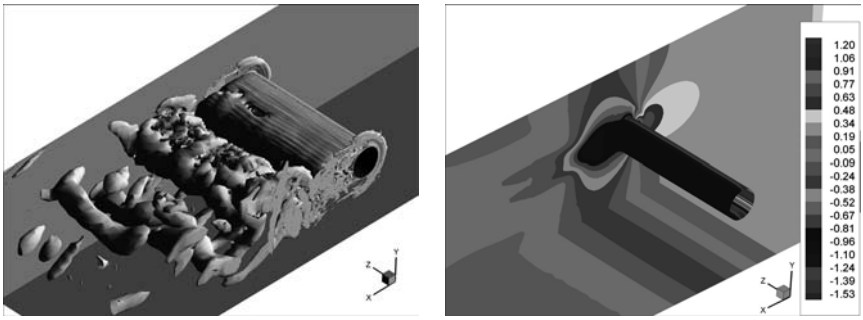

Figure 1 Instantaneous swirl (λ_2=0.5) isosurface (left) and time averaged pressure field (right) from SA DES of the 3D cylinder flow (Test Case 21)

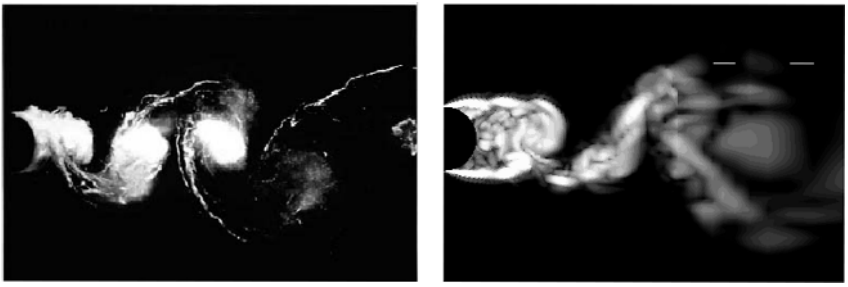

Figure 2 Comparison of flow visualisations from the SA DES (right) and IMFT experiment (left)

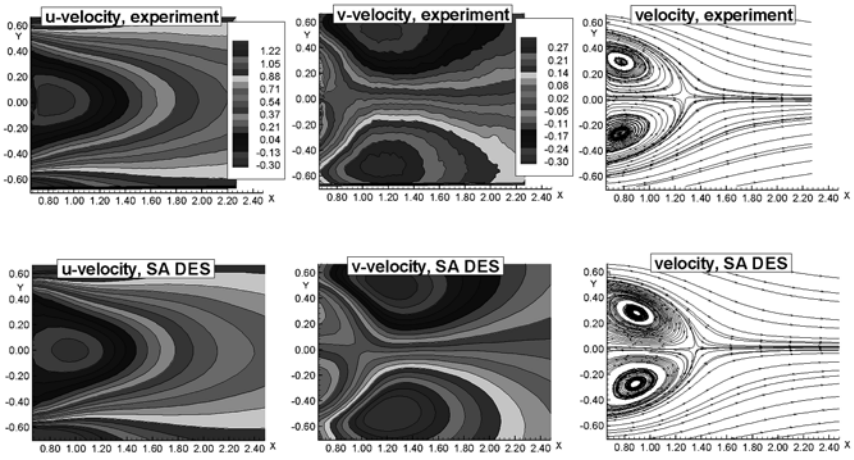

Figure 3 Comparison of SA DES mean flow prediction with IMFT experiment

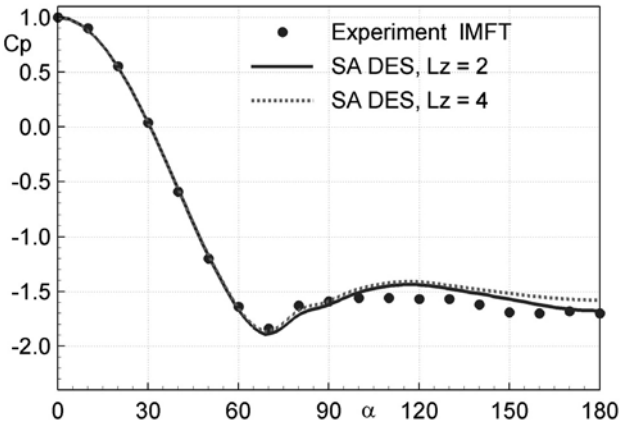

Figure 4 Comparison of SA DES prediction of mean pressure distribution over the cylinder with IMFT experiment

15.3 3D RANS of the ONERA A-Airfoil (TC 28): evaluation of sidewall effect

A goal of this study was getting an estimation of possible effect of the sidewalls on the flow past the A-airfoil studied in the experiments of Gleyzes and Capbern, 2003. In order to reach this objective we have performed 3D steady RANS computations of the flow past the airfoil with account of the sidewalls of the test section. The turbulence models used in these computations are: SA, SARC, and SST. The problem set-up reproduced the experimental set-up in terms of the Reynolds number ($Re=2.1\cdot10^6$), Mach number (0.15), angle of attack (13 degrees), test section geometry, and incoming boundary layer parameters.

In the experiment, the flow at the considered angle of attack turns out to be virtually 2D. In contrast to that, CFD, no matter which of the three listed above turbulence models is used, predicts a massive separation of the flow in the area of the airfoil/sidewall junction. This is clearly seen in Fig. 5, where we compare the experimental (oil flow) and computational (wall streamlines) flow visualisations.

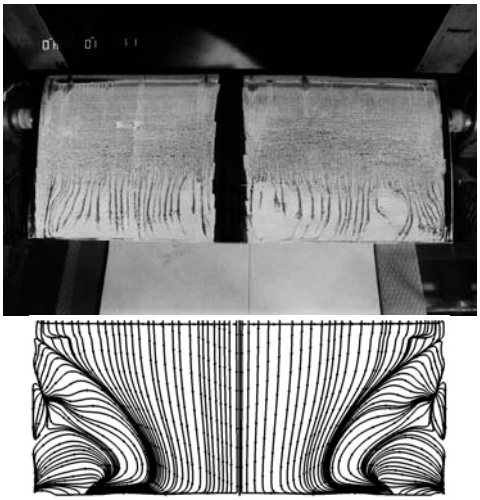

Figure 5 Comparison of experimental (up) and computational (down) flow visualisations

Figure 6 gives a more detailed idea on the flow topology predicted by 3D RANS, which clearly shows the large corner separation zones forming in the airfoil/sidewall corner due to the adverse pressure gradient on the suction side of the airfoil.

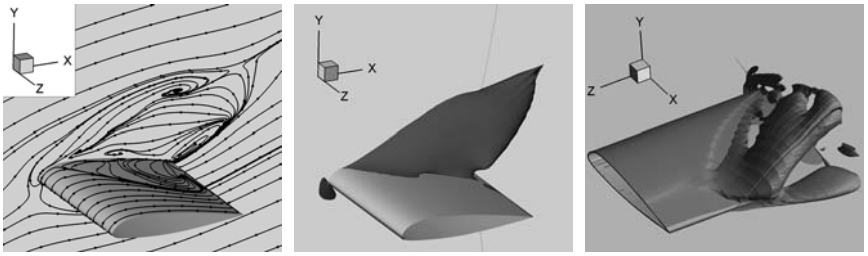

Figure 6 Streamlines at the airfoil surface and sidewall (left), surface of zero streamwise velocity (middle), and swirl isosurface λ_2=1.4 from 3D RANS solution

As a result, all the characteristics of the flow predicted by 3D RANS are far from those measured in the experiment and, also, from the similar predictions of 2D RANS (see Fig. 7).

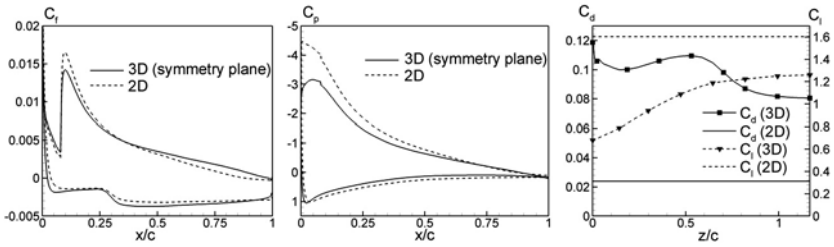

Figure 7 Comparison of the friction (left) and pressure (middle) coefficients distributions over the airfoil at symmetry plane from 3D RANS with 2D RANS predictions and spanwise distributions of drag and lift coefficients from 3D RANS (right)

As of today, we cannot find any quite definite explanation of this contradiction. It might be cased by an inadequate performance of the linear eddy-viscosity RANS models in this type of flow. A more optimistic explanation suggested by F. Menter in the course of the discussion of the results presented above is that we might be just near a bifurcation point, i.e., that with the same problem set-up but different initial conditions one could get different solution. A test would be to compute the flow at different angles of attack and see if there is a hysteresis when approaching the 13 degrees from below or from above, and at which angle the flow topology changes.